Braz J Phys (2011) 41:113–117
DOI 10.1007/s13538-011-0020-7

SOCIEDADE BRASILEIRA DE FÍSICA

CONDENSED MATTER

Growth of ZnO Nanostructures on Porous Silicon and Oxidized Porous Silicon Substrates

M. Rajabi · R. S. Dariani · A. Iraji zad

Received: 6 October 2010 / Published online: 17 May 2011

Abstract We have investigated an oxidation of substrate effect on structural morphology of zinc oxide (ZnO) rods. ZnO rods are grown on porous silicon (PS) and on thermally oxidized porous silicon substrates by carbothermal reduction of ZnO powder through chemical vapour transport and condensation. Porous silicon is fabricated by electrochemical etching of silicon in hydrofluoric acid solution. The effects of substrates on morphology and structure of ZnO nanostructures have been studied. The morphology of substrates is studied by atomic force microscopy in contact mode. The texture coefficient of each sample is calculated from X-ray diffraction data that demonstrate random orientation of ZnO rods on oxidized porous silicon substrate. The morphology of structures is investigated by scanning electron microscopy that confirms the surface roughness tends to increase the growth rate of ZnO rods on oxidized PS compared with porous silicon substrate. A green emission has been observed in ZnO structures grown on oxidized PS substrates by photoluminescence measurements.

Keywords ZnO · Porous silicon · XRD · Texture coefficient · Chemical vapour transport and condensation

M. Rajabi · R. S. Dariani (✉)
Department of Physics, Alzahra University, Tehran, 19938-91176, Iran
e-mail: sabetdariani@gmail.com

A. Iraji zad
Department of Physics, Sharif University of Technology, Tehran, 11365-11155, Iran

1 Introduction

In recent years, semiconductor nanostructures have attracted much attention because of their unique properties and potential applications in electronic and optoelectronic devices [1, 2]. One of the most interesting compound semiconductors is zinc oxide (ZnO). It is a wide-bandgap semiconductor with a direct bandgap of 3.37 eV and a high exciton binding energy of 60 meV at room temperature with a diverse group of growth morphologies such as nanowires, nanorods, nanotubes, nanocages, nanobelts and nanocombs [3]. In this group of morphologies, nanowires and nanorods have been widely used in optoelectronic devices such as solar cells and photodetectors due to their facility for electron transport [4, 5]. ZnO's properties and its applications in optoelectronic devices have been reviewed [6]. In some optoelectronic devices like photoconductors, these materials should be grown on a high resistive substrate. Silicon is the most extensively used substrate for growth of one-dimensional ZnO nanostructures because of its low cost compared with other substrates such as sapphire. Also, the SiO_2, as an amorphous substrate, has obvious technological advantages and potential applications [7]. The other high resistive substrates are porous silicon (PS) and oxidized porous silicon which could be the interesting substrates for production of nanostructure materials especially ZnO nanowires [8]. PS is a silicon nanostructure which is fabricated by electrochemical etching of silicon in hydrofluoric acid (HF) solution. The observation of strong room temperature visible photoluminescence (PL) from PS and blue emission due to quantum confinement or presence of nanocrystals and large surface area makes it a promising material for Si-based optoelectronic devices

[9]. It is believed that the rough surface morphology of porous silicon has advantages for the growth of nanowires by reducing its strain and increasing the number of nuclei sites [10–12]. Separation of PS layer from silicon substrate is possible through layer transfer techniques which provide the opportunity to reuse the Si substrate [13]. A variety of methods have been used to grow ZnO nanolayers and nanowires on porous silicon substrate, such as hydrothermal method, sol–gel method, spray technique, magnetron sputtering and vapour phase transport method [14–18]. The last method involves generation of Zn or Zn suboxide by carbothermal reduction of ZnO. Then the vapour is transported onto a substrate placed downstream of carrier gas where it condenses and deposits through vapour–solid or vapour–liquid–solid mechanism. For the first time, Chang et al. [19] investigated the growth and characterization of ZnO nanowires grown on the surface of porous silicon without any catalyst. Hsu et al. [10] reported an orientation enhancement for ZnO nanowires with controlled size porous silicon substrates by vapor–liquid–solid process. Yu et al. [20–22] studied the synthesis, field emission and optical property of ZnO nanostructures with different morphologies on CuO-catalyzed porous silicon substrates. To our knowledge, there have been no reports on growth of ZnO on oxidized PS which can act as a substrate of photoconductors. The use of PS layer separated from Si as a freestanding substrate is difficult because it is very friable. The oxidation process can make it sturdier.

In this paper, we report the growth of ZnO rods on porous silicon and oxidized porous silicon using vapour-phase transport method and study the effect of substrate on growth process. We investigate the effect of oxidation process on porous silicon using atomic force microscopy (AFM) and the structural quality of ZnO rods by using the top view and cross-sectional scanning electron microscopy (SEM) and X-ray diffraction (XRD) analysis. The photoluminescence properties of ZnO nanostructures grown on oxidized PS are investigated, as well.

2 Experiments

In this study, we use (100) oriented, boron-doped p-type silicon wafers with resistivity of 1–5 Ωcm and thickness of 525 ± 20 μm. The preparation of samples involves two steps: First, the preparation of substrates included PS and oxidized PS and, second, growth of ZnO rods by vapour-phase transport method. The porous layer is formed by electrochemical etching of Si wafer at a constant current density of 20 mA/cm^2 for 20 min in ethanoic solution of 32% HF ($HF/C_2H_5OH = 4{:}1$). The details of setup and method of PS formation are reported elsewhere [23]. Oxidation of porous silicon is performed by annealing at 800°C for 1 h in an ambient air furnace.

ZnO rods are grown in a horizontal quartz tube furnace. One side of the quartz tube is connected to N_2 gas inlet and the other side to the environment. The distance between the gas inlet and centre of furnace is about 55 cm. Source material is a mixture of zinc oxide powder (99%, Merck) and graphite powder (99%, LOBA Chemie) with equal amounts (a weight ratio of 1:1). The source material and substrate are placed into a small quartz tube (2.7 cm inner diameter and 20 cm length). This tube is transferred into the outer quartz tube (3.8 cm inner diameter and 95 cm length) of a horizontal furnace. The substrate is placed at different distances from the source material downstream along the direction of gas flow, which resulted in different substrate temperatures due to the natural temperature gradient along the furnace. The source material, which is placed at the central hot zone of the furnace, is heated to 1,000°C at a rate of 20°C/min and is kept at this temperature for 1 h under constant flow of high purity nitrogen gas at a rate of 200–300 sccm. Then, the furnace is turned off to be cooled down to room temperature. Under these conditions, the substrate temperature during growth process is determined to be 890 ± 10°C.

The crystal structure and surface morphology of ZnO rods are characterized by XRD (Philips X' Pert) with CuK_α radiation ($\lambda = 0.1542$ nm), SEM (Philips XL30) and AFM (Veeco-Termo Microscopes) in contact mode. The photoluminescence measurements are made at room temperature using a UV lamp and a filter centred at a wavelength of 254 nm and UV–visible (Avantes-2048Tec) Spectrometer.

3 Results and Discussions

Figure 1a, b shows the top view and cross-sectional SEM images of ZnO structures grown on porous silicon substrates. The images indicate the formation of large islands which have no specific epitaxial arrangement and nanorods and nanobelts grown on island surfaces and boundaries observed in a higher magnification SEM images. The table related to energy dispersive X-ray (EDX) spectrum in Fig. 1c confirms the formation of ZnO structures on PS substrate. The random orientation and higher growth rate of rods grown on oxidized PS were observed in the top view and cross-sectional SEM images of Fig. 2 compare with PS substrate. The cross-sectional SEM image of rods grown on oxidized

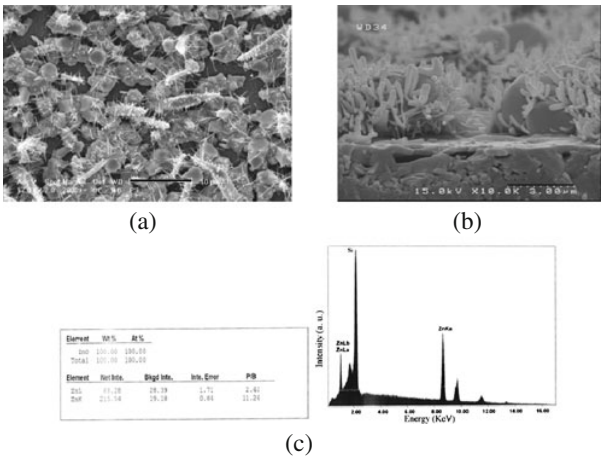

Fig. 1 **a** Top view and **b** cross-sectional SEM images of ZnO structures grown on porous silicon and **c** EDX spectrum of single ZnO island on PS. The *scale bar* in **a** and **b** represents 10 and 3 μm, respectively

PS indicates that the oxide layer is thick enough and it is possible to separate from silicon substrate as a freestanding substrate for application in photodetector devices.

Figure 1c displays an EDX spectrum from the top of one single island. It reveals the presence of Zn and Si. The silicon peak is related to porous silicon substrate and the structures are zinc oxide. The irregular shape and large size of structures are the results of high supersaturation and growth temperature [24]. At lower temperatures, nanowires and rods can grow on both substrates.

In order to verify the crystal structure and determine the differences, the X-ray diffraction analyses were carried out in the 30–80° range of 2θ. Figure 3 shows the diffraction patterns of ZnO structures grown on PS and oxidized PS substrates. All the diffraction peaks in the spectra are indexed to the hexagonal-wurtzite structure of ZnO. Table 1 presents the lattice constants of each sample that are calculated from the XRD patterns.

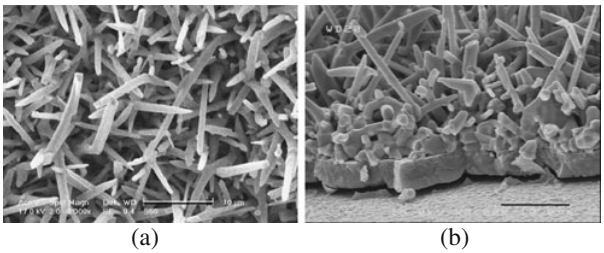

Fig. 2 **a** Top view and **b** cross-sectional SEM images of ZnO rods grown on oxidized porous silicon. The *scale bar* is 10 μm

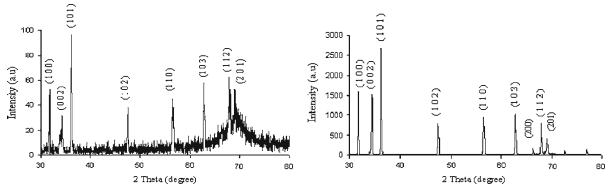

Fig. 3 X-ray diffraction of ZnO nanostructures deposited under same growth conditions on **a** PS substrate and **b** oxidized PS substrate

They are in good agreement with the standard data, i.e. $a = 3.2539$ Å and $c = 5.2098$ Å (JCPDS card 80-0075) especially for the structures grown on the oxidized PS, within experimental error. In the XRD pattern of ZnO structures grown on PS substrate except SiO_2 peaks from porous silicon, we observe peaks related to zinc silicate oxide. This observation reveals that zinc silicate oxide can be a polycrystalline wetting layer initially formed by Zn and Zn sub oxides (ZnO_x, $x < 1$). Then, the rough surface of PS act as a nucleation sites [19]. In the XRD patterns, no diffraction peaks from Zn or other phases were observed.

The observed XRD patterns of ZnO structures grown on PS (Fig. 3a) and oxidized PS (Fig. 3b) show a similar coincidence to the standard pattern for powder. To determine the preferred orientation of structures grown on both substrates, the texture coefficient of the diffraction peaks is calculated and listed in Table 2. The texture coefficient of (hkl) plane (TC(hkl)) is defined as the following expression [13]:

$$\mathrm{TC(hkl)} = \frac{I_{(\mathrm{hkl})}/I_{\mathrm{o}(\mathrm{hkl})}}{N^{-1}\sum_{N} I_{(\mathrm{hkl})}/I_{\mathrm{o}(\mathrm{hkl})}} \tag{1}$$

where $I_{(\mathrm{hkl})}$ is the measured intensity, $I_{\mathrm{o}(\mathrm{hkl})}$ is the standard intensity of (hkl) plane taken from the JCPDS data and N is the total number of diffraction peaks. For a sample with randomly oriented crystallite, TC(hkl) is equal to 1. When this value is larger than 1, a preferred orientation exists along the (hkl) plane.

These results (Table 2) show random orientation of ZnO rods on the oxidized PS substrate. The structures grown on PS have preferred growth orientation along (112) and (201) planes.

Table 1 The calculated values of lattice constants

Substrate	a (Å)	c (Å)
PS	3.2515	5.2142
Oxidized PS	3.2537	5.2094

Table 2 The calculated values of TC for different ZnO diffraction peaks

	(110)	(002)	(101)	(102)	(110)	(103)	(200)	(112)	(201)
PS	0.38	0.68	1	1.16	1.19	1.27	1.40	1.74	1.73
Oxidized PS	0.83	1	0.74	0.89	0.83	1.12	0.89	0.94	1.03

The surface morphology difference of PS and oxidized PS can be the result of higher growth rate of ZnO rods on oxidized PS substrate at the same growth conditions. SEM analysis of porous silicon and oxidized PS surface does not show any considerable change in the structure. Also, it is difficult to observe nanoporous silicon pores due to small size. Surface analysis by AFM is performed in contact mode in order to determine the surface differences of PS and oxidized PS surface which can affect the ZnO growth process. Figure 4 shows two- and three-dimensional AFM images of porous silicon and oxidized PS for a scanning area of 3×3 μm^2. For porous silicon, the value of the root mean square roughness, the average roughness and mean height of surface are 6.31, 4.56 and 35.77 nm and for oxidized PS are 14.72, 11.62 and 58.12 nm, respectively, which are obtained by the AFM images. The results show that the oxidation process leads to evolution of surface roughness and mean height of oxidized PS compared with PS.

The growth mechanism for the same growth condition is obviously different on PS and oxidized PS substrates which could be a result of different surface morphologies of substrates. It is known that the sites with a higher surface energy act as nucleation sites. The AFM analyses indicate that the rough surface of oxidized PS can provide more nucleation sites for growth of initial ZnO islands.

According to the above results, we can explain the formation models of nano- and microrods. At the beginning, the Zn or ZnO_x ($x < 1$) species are randomly deposited on substrate surface and formed a polycrystalline wetting layer. For ZnO rods grown on PS at the high growth temperature (~890°C), the deposited particles have sufficient diffusion length, which is lower than diffusion length on silicon substrate (because of the rough surface of PS), to move along substrate surface to form large ZnO islands as observed in the top view and cross-sectional SEM images (Fig. 1a, b). On the other hand, the surface defects and their boundaries act as the nucleation sites for growth of micro- or nanorods.

The growth of ZnO rods on oxidized PS layer is relatively easy compared with PS substrate because of higher surface roughness. The rough surface limits the diffusion of adatoms, thus forms smaller island on substrate surface.

It is known that ZnO is a luminescent material. Usually two emission bands are observed in PL spectrum: a visible blue green band related to deep level defects, such as oxygen vacancies and Zn interstitials, and a narrow UV emission due to exciton recombination near band edge. It has been suggested that these two emission bands are in competition with each other, and high crystallinity structure enhances the UV emission [6]. Figure 5 shows the room temperature PL spectra of ZnO samples grown on oxidized porous silicon

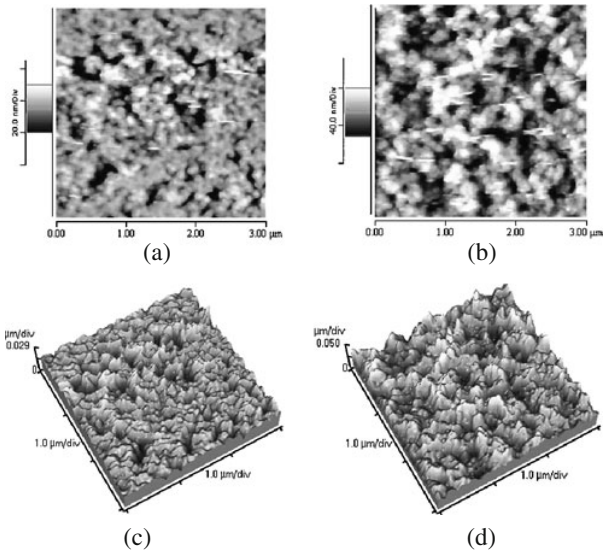

Fig. 4 Two- and three-dimensional AFM images of **a**, **c** porous silicon and **b**, **d** oxidized PS

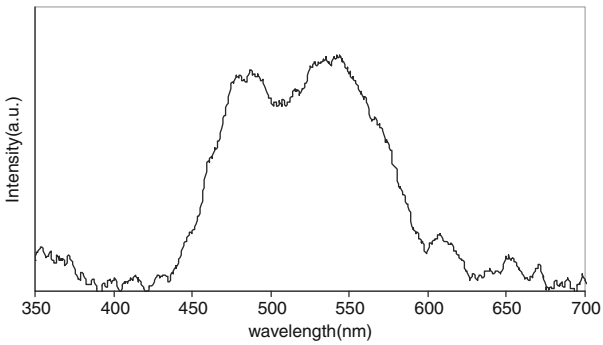

Fig. 5 Room temperature PL spectra of ZnO structures grown on the oxidized PS substrates

substrate, a green emission bands centred at around 490 and 545 nm. The proposed hypothesis relates these visible emission bands to oxygen vacancies [25, 26]. The absence of UV emission band could be the results of structural defects as proposed by Sieber et al. [27]. ZnO structures grown on PS substrate do not show any detectable PL as a result of low density of rods on PS surface.

4 Conclusions

We have studied the effect of surface roughness on structural morphology of ZnO rods grown on porous silicon and oxidized porous silicon substrate by carbothermal reduction of ZnO. The AFM results indicate that the oxidation process leads to higher surface roughness of oxidized porous silicon substrate than PS substrate. The texture coefficient calculated from XRD data and SEM images show the random orientation of ZnO nanorods grown on oxidized porous layer. Comparison of structure and morphology of ZnO nanostructures grown on oxidized porous silicon substrate with nanostructures formed on porous silicon substrate demonstrates the higher growth rate on oxidized PS. Also, it might be possible to separate ZnO rods grown on oxidized porous silicon from the silicon substrates, a possibility that calls for more study.

References

1. T. Zhai, X. Fang, M. Liao, X. Xu, H. Zeng, B. Yhshio, D. Golberg, Sensors **9**, 6504–6529 (2009)
2. L. Tsakalakos, Mater. Sci. Eng. R **62**, 175–189 (2008)
3. Z.L. Wang, J. Phys.: Condens. Matter **16**, R829–R858 (2004)
4. Y. Hsu, Y.Y. Xi, A.B. Djurisic, W.K. Chan, Appl. Phys. Lett. **92**, 133507 (2008)
5. K.J. Chen, F.Y. Hung, S.J. Chang, S.J. Young, J. Alloys Compd. **479**, 674–677 (2009)
6. A.B. Djurisic, A.M.C. Ng, X.Y. Chen, Prog. Quantum Electron. **34**, 191–259 (2010)
7. S. Guha, N.A. Bojarczuk, Appl. Phys. Lett. **73,** 1487–1489 (1998)
8. C. Soci, A. Zhang, B. Xiang, S.A. Dayeh, D.P. Dayeh, D.P.R. Aplin, J. Park, X.Y. Bao, Y.H. Lo, D. Wang, Nano Lett. **7**, 1003–1009 (2007)
9. L.T. Canham, Appl. Phys. Lett. **57**, 1046–1048 (1990)
10. H.C. Hsu, C.S. Cheng, C.C. Chang, S. Yang, C.S. Chang, W.F. Hsieh, Nanotechnology **16**, 297–301 (2005)
11. J.S. Lee, M.I. Kang, S. Kim, M.S. Lee, Y.K. Lee, J. Cryst. Growth **249**, 201–207 (2003)
12. P. Yang, C.M. Lieber, J. Mater. Res. **12**, 2981–2996 (1997)
13. C.S. Solanki, R.R. Bilyalov, J. Poortmans, J. Nijs, R. Mertens, Sol. Energy Mater. Sol. Cells **83**, 101–113 (2004)
14. J.P. Kar, M.H. Ham, S.W. Lee, J.M. Myoung, Appl. Surf. Sci. **255**, 4087–4092 (2009)
15. R.G. Singh, F. Singh, V. Agarwal, R.M. Mehra, J. Phys. D: Appl. Phys. **40**, 3090–3093 (2007)
16. C. Shaoqiang, Z. Jian, F. Xiao, W. Xiahua, L. Laiqiang, S. Yanling, X. Qingsong, W. Chang, Z. Jianzhong, Z. Ziqiang, Appl. Surf. Sci. **241**, 384–391 (2008)
17. H. Elhouichet, M. Oueslati, Mater. Sci. Eng. B **79**, 27–30 (2001)
18. P. Prabarkaran, M. Peres, T. Monteiro, E. Fortunato, R. Martins, I. Ferreira, J. Non-Cryst. Solids **345**, 2181–2185 (2008)
19. C.C. Chang, C.S. Chang, Jpn. J. Appl. Phys. **43**, 8360–8364 (2004)
20. K. Yu, Y. Zhang, L. Luo, W. Wang, Z. Zhu, J. Wang, Y. Cui, H. Ma, W. Lu, Appl. Phys. A **79**, 443–446 (2004)
21. K. Yu, Y. Zhang, L. Luo, S. Ouyang, H. Geng, Z. Zhu, Mater. Lett. **59**, 3525–3529 (2005)
22. K. Yu, Y. Zhang, R. Xu, D, Jiang, L. Luo, Q. Li, Z. Zhu, W. Lu, Solid State Commun. **133**, 43–47 (2005)
23. M. Rajabi, R.S. Dariani, J. Porous Mater. **16**, 513–519 (2009)
24. C. Ye, X. Fang, Y. Hao, X. Teng, L. Zhang, J. Phys. Chem. B **109**, 19758–19765 (2005)
25. M.K. Patra, K. Manzoor, M. Manoth, S.P. Vadera, N. Kumar, J. Lumin. **128**, 267–272 (2008)
26. A. van Dijken, E.A. Meulenkamp, D. Vanmaekelbergh, A. Meijerink, J. Phys. Chem. B **104**, 1715–1723 (2000)
27. B. Sieber, A. Addad, S. Szunerits, R. Boukherroub, J. Phys. Chem. Lett. **1**, 3033–3038 (2010)